# A Model For Hydrogen Thermal Conductivity and Viscosity Including The Critical Point

Howard A. WAGNER[+], Gokturk TUNC[‡] and Yildiz BAYAZITOGLU[‡]

## Abstract

In order to conduct a thermal analysis of heat transfer to liquid hydrogen near the critical point, an accurate understanding of the thermal transport properties is required. A review of the available literature on hydrogen transport properties identified a lack of useful equations to predict the thermal conductivity and viscosity of liquid hydrogen. The tables published by the National Bureau of Standards were used to perform a series of curve fits to generate the needed correlation equations. These equations give the thermal conductivity and viscosity of hydrogen below 100 K. They agree with the published NBS tables, with less than a 1.5 percent error for temperatures below 100 K and pressures from the triple point to 1000 KPa. These equations also capture the divergence in the thermal conductivity at the critical point.

**Key Words:** *Hydrogen, Thermal Conductivity, Viscosity, Critical point, Curve-fit*

## Introduction

Typical analytical forms of the equation of state predict finite values for the specific heats $C_p$ and $C_v$, the thermal conductivity, and the speed of sound at the critical point. It is well established by experimental results that the specific heats and the thermal

[+] NASA Johnson Space Center, Houston, TX 77058
[‡] Mechanical Engineering and Materials Science Department, Rice University, Houston, TX 77005

conductivity diverge to infinity as the critical point is approached. Garland and Williams [1] studied the speed of sound in xenon near its critical point. The speed of sound varies as $\frac{1}{\sqrt{C_v}}$. Therefore, as $C_v$ goes to infinity near the critical point, the speed of sound will go to zero. They show that although the speed of sound approaches zero at the critical temperature, it is still larger than 10 m/s for $\frac{(T - T_c)}{T_c} > 10^{-9}$. The speed of sound going to zero at the critical point is common to all fluids.

The use of empirical equations of state is required to adequately model the change in the fluid properties near the critical point. Hendricks et al. [2] developed a computer program to provide the thermophysical properties of ten different cryogenic fluids. The program did not attempt to model the anomalous behavior near the critical point, and therefore could not be utilized for research in critical point heat transfer. Emanuel [3] applied critical point theory to predict the thermodynamic properties of a real fluid near the critical point. The theory is applicable to any fluid and accurately predicts the divergence of the properties of interest at the critical point. The use of critical point theory needs further investigation and is beyond the scope of this research. Nwobi et al. [4] recently used molecular dynamics theory to predict the thermodynamic properties of supercritical oxygen. The approach accurately predicts the divergence of certain important properties near the critical point, but is much too time intensive to be of any practical use in numerical simulations.

In 1980, the National Bureau of Standards (NBS) [5] created a computer program for the NASA Johnson Space Center to predict the thermophysical properties for fifteen cryogenic fluids. The program accurately reproduces the divergence of the fluid

properties at the critical point. The output from the program was compared to the published tables from the NBS with very close correlation, often within 1% of the tabulated values. This program did not include the thermal conductivity and viscosity of hydrogen. A review of previous reports from the NBS [6,7] on the thermal conductivity and viscosity of liquid hydrogen failed to provide any useful equations to predict these two transport properties. A decision was made to perform a series of curve fits using the published values from the NBS.

**Thermal Conductivity**

The NBS tables [8] were used to curve fit the thermal conductivity of gaseous and liquid hydrogen. The curve fits are valid for temperatures from the triple point to 100 K and pressures to 1000 KPa. For temperatures below 100 K, the thermal conductivity data were fitted to a modified Enskog theory using Eq. (1).

$$k = \exp(Z + \exp(B) * \rho + C * \rho^2) \qquad (1)$$

where the coefficients are given as

$$Y = \ln(T)$$

$$Z = X_1 + X_2 * Y + X_3 * Y^2 + X_4 * Y^3 + X_5 * Y^4$$

$$B = X_6 + X_7 * Y + X_8 * Y^2 + X_9 * Y^3 + X_{10} * Y^4 + X_{11} * Y^5$$

$$C = X_{12} + X_{13} / T + X_{14} / T^2 + X_{15} / T^3 + X_{16} / T^4$$

This form of the modified Enskog equation was used to predict the thermal conductivity of helium [9]. Since the properties of hydrogen are close to those of helium it was decided to use the same form of the modified Enskog equation to predict the thermal conductivity of hydrogen. The temperature, T, is in degrees Kelvin and the

density, $\rho$, is in $g/cm^3$. Thermal conductivity, k, is given in W/m-K. The resulting curve fit coefficients are given as

| | |
|---|---|
| X1 = 0.383546x10 + 01 | X2 = - 0.123663x10 + 02 |
| X3 = 0.611632x10 + 01 | X4 = - 0.123492x10 + 01 |
| X5 = 0.922390x10 - 01 | X6 = 0.569497x10 + 02 |
| X7 = - 0.682941x10 + 02 | X8 = 0.348056x10 + 02 |
| X9 = - 0.884876x10 + 0 | X10 = 0.112028x10 + 01 |
| X11 = - 0.568872x10 - 01 | X12 = 0.473430x10 + 02 |
| X13 = - 0.300763x10 + 04 | X14 = 0.776719x10 + 05 |
| X15 = 0.106809x10 + 07 | X16 = 0.888314x10 + 06 |

The average error was 0.046% and the standard deviation was 4.35%. A three-sigma spread on the data would give an estimated 13% error. The maximum error differs by 99% from the published tables near the critical point. Far away from the critical point the error is generally less than 0.5%. The results from Eq. (1) showed very good correlation at the higher densities.

The difference between the values predicted by Eq. (1) and the published values demonstrated a seventh order polynomial relationship based on density for constant temperature conditions. This relationship leads to the use of seventh order polynomials for density and cubic polynomials for temperature to correct for the lower density conditions. The resulting form of the correction term is given by Eq. (2).

$$Corr = A + B*\rho + C*\rho^2 + D*\rho^3 + E*\rho^4 + F*\rho^5 + G*\rho^6 + H*\rho^7 \qquad (2)$$

where the coefficients are given as

$$A = X_1 + X_2*T + X_3*T^2 + X_4*T^3$$

$$B = X_5 + X_6*T + X_7*T^2 + X_8*T^3$$

$$C = X_9 + X_{10} * T + X_{11} * T^2 + X_{12} * T^3$$

$$D = X_{13} + X_{14} * T + X_{15} * T^2 + X_{16} * T^3$$

$$E = X_{17} + X_{18} * T + X_{19} * T^2 + X_{20} * T^3$$

$$F = X_{21} + X_{22} * T + X_{23} * T^2 + X_{24} * T^3$$

$$G = X_{25} + X_{26} * T + X_{27} * T^2 + X_{28} * T^3$$

$$H = X_{29} + X_{30} * T + X_{31} * T^2 + X_{32} * T^3$$

The coefficients of the density correction for different temperature and density ranges are given in Table 1. The final form of the equation for thermal conductivity is the sum of Eqs. (1) and (2). The results are summarized in Table 2.

The critical point enhancement was applied to the thermal conductivity in the temperature range $32.95\text{K} \le T \le 33\text{K}$ and the density range $0.02 < \rho \le 0.04\text{g/cm}^3$. The critical point enhancement was calculated by Eq. (3).

$$\text{Crit} = 41.20535 * \exp(-6675067 * (\rho - 0.031428)^2 - 2.0\text{x}10^7 * (T - 32.976)^2) \qquad (3)$$

Figure 1 shows the maximum error between the calculated values and the values given by the NBS tables for temperatures below 100 K. The data fall below a 1.6% error, with the majority well below 1%. The curve fit was then compared to the tabular values for three significant pressures: atmospheric, critical, and super-critical. Figure 2 compares the predicted thermal conductivity to the published values for hydrogen at one atmosphere pressure. The predicted values closely match the published values for both the liquid and gaseous phases. The correlation at the critical pressure is presented in Figure 3. The curve fit results accurately capture the divergence at the critical point. The

divergence is limited to a very narrow temperature range. Finally, the correlation at a supercritical pressure is shown in Figure 4. Here the pressure was set to 1500 KPA or 1.16 times the critical pressure. From the shape of the curve it is obvious why three density ranges were required to provide an acceptable curve fit. The resulting equations still capture the divergence near the critical point. The magnitude of the critical point divergence decreases as the pressure is increased.

**Viscosity**

The same NBS tables [8] were used to curve fit the viscosity of hydrogen. The curve fits are valid for temperatures from the triple point to 100 K and pressures to 1000 KPa.

In the temperature range $65K < T \leq 100K$ the data were fitted using Eq. (4).

$$\mu = A + B*\rho + C*\rho^2 + D*\rho^3 + E*\rho^4 + F*\rho^5 \qquad (4)$$

where the coefficients are given as

$$A = 0.113414x10^{-06} + 0.524985x10^{-07} * T - 0.115124x10^{-09} * T^2$$

$$B = 0.232625x10^{-03} - 0.453684x10^{-05} * T + 0.244673x10^{-07} * T^2$$

$$C = -0.245986x10^{-01} + 0.551425x10^{-03} * T - 0.295357x10^{-05} * T^2$$

$$D = 0.101041x10^{+01} - 0.218787x10^{-01} * T + 0.115788x10^{-03} * T^2$$

$$E = -0.156836x10^{+02} + 0.338478x10^{+00} * T - 0.177112x10^{-02} * T^2$$

$$F = 0.856032x10^{+02} - 0.180672x10^{+01} * T + 0.933153x10^{-02} * T^2$$

The temperature, T, is in degrees Kelvin and the density, $\rho$, is in $g/cm^3$. Viscosity, $\mu$, is in Poise. The average error was 0.0013% and the standard deviation was

0.32%. A three-sigma spread on the data would give an estimated 0.96% error. The maximum error for this range was 1.62%.

In the temperature range $46\,\mathrm{K} < T \leq 65\,\mathrm{K}$ the data were fitted using Eq. (5).

$$\mu = A + B*\rho + C*\rho^2 + D*\rho^3 + E*\rho^4 + F*\rho^5 + G*\rho^6 + H*\rho^7 \qquad (5)$$

where the coefficients are given as

$$A = 0.542644\text{x}10^{-06} + 0.384834\text{x}10^{-07} * T + 0.373781\text{x}10^{-11} * T^2$$

$$B = -0.382474\text{x}10^{-03} + 0.156988\text{x}10^{-04} * T - 0.144832\text{x}10^{-06} * T^2$$

$$C = 0.648002\text{x}10^{-01} - 0.262206\text{x}10^{-02} * T + 0.249320\text{x}10^{-04} * T^2$$

$$D = -0.343722\text{x}10^{+01} + 0.152163\text{x}10^{+00} * T - 0.149907\text{x}10^{-02} * T^2$$

$$E = 0.824312\text{x}10^{+02} - 0.404907\text{x}10^{+01} * T + 0.415405\text{x}10^{-01} * T^2$$

$$F = -0.906190\text{x}10^{+03} + 0.528978\text{x}10^{+02} * T - 0.573267\text{x}10^{+00} * T^2$$

$$G = 0.376977\text{x}10^{+04} - 0.319712\text{x}10^{+03} * T + 0.377532\text{x}10^{+01} * T^2$$

$$H = 0.467651\text{x}10^{+00} + 0.656682\text{x}10^{+03} * T - 0.916660\text{x}10^{+01} * T^2$$

The average error was 0.031% and the standard deviation was 0.25%. A three-sigma spread on the data would give an estimated 0.78% error. The maximum error for this range was 1.53%.

For $T \leq 46\,\mathrm{K}$ and $\rho \leq 0.075\,\mathrm{g/cm^3}$ the data were fitted using Eq. (6).

$$\mu_{LD} = A + B*\rho + C*\rho^2 + D*\rho^3 + E*\rho^4 \qquad (6)$$

where the coefficients are given as

$$A = X_1 + X_2 * T + X_3 * T^2 + X_4 * T^3 + X_5 * T^4$$

$$B = X_6 + X_7 * T + X_8 * T^2 + X_9 * T^3 + X_{10} * T^4$$

$$C = X_{11} + X_{12} * T + X_{13} * T^2 + X_{14} * T^3 + X_{15} * T^4$$

$$D = X_{16} + X_{17} * T + X_{18} * T^2 + X_{19} * T^3 + X_{20} * T^4$$

$$E = X_{21} + X_{22} * T + X_{23} * T^2 + X_{24} * T^3 + X_{25} * T^4$$

where,

| | |
|---|---|
| X1 = 0.189281x10 - 06 | X2 = 0.130968x10 - 07 |
| X3 = 0.277990x10 - 08 | X4 = - 0.721669x10 - 10 |
| X5 = 0.599499x10 - 12 | X6 = 0.266869x10 - 03 |
| X7 = - 0.219076x10 - 04 | X8 = 0.541725x10 - 06 |
| X9 = - 0.255997x10 - 08 | X10 = - 0.317459x10 - 10 |
| X11 = 0.732495x10 - 01 | X12 = - 0.744391x10 - 02 |
| X13 = 0.302109x10 - 03 | X14 = - 0.553316x10 - 05 |
| X15 = 0.380544x1007 | X16 = - 0.262958x10 + 01 |
| X17 = 0.266919x10 + 00 | X18 = - 0.105438x10 - 01 |
| X19 = 0.187012x10 - 03 | X20 = - 0.124540x10 - 05 |
| X21 = 0.229229x10 + 02 | X22 = - 0.228625x10 + 01 |
| X23 = 0.891753x10 - 01 | X24 = - 0.156164x10 - 02 |
| X25 = 0.102719x10 - 04 | |

The average error was 0.078% and the standard deviation was 0.54%. A three-sigma spread on the data would give an estimated 1.70% error. The maximum error for this range was 2.39%.

This same equation was used to extrapolate into the higher density region. A density correction term was calculated to reduce the magnitude of the error. The final form of the equation for viscosity is the sum of the two terms, $\mu = \mu_{LD} + \mu_{HD}$ ($\mu_{HD}$ is obtained by substituting the correction coefficients into Eq. (6)). The coefficients of the

density correction term are as given below for different temperature and density ranges. The effects of correction for these cases are given in Table 3.

In the temperature range $40\text{K} < \text{T} \leq 46\text{K}$ and $\rho > 0.075\text{g/cm}^3$, the definition of the coefficients was changed to reflect a linear relationship in temperature in place of the previous quadratic temperature relationship. The coefficients are now defined as

$$A = 0.296606\text{x}10^{-01} - 0.599524\text{x}10^{-03} * \text{T}$$

$$B = -0.141972\text{x}10^{+01} + 0.285903\text{x}10^{-01} * \text{T}$$

$$C = 0.254884\text{x}10^{+02} - 0.511198\text{x}10^{+00} * \text{T}$$

$$D = -0.203521\text{x}10^{+03} + 0.406355\text{x}10^{+01} * \text{T}$$

$$E = 0.610254\text{x}10^{+03} - 0.121242\text{x}10^{+02} * \text{T}$$

**$36\text{K} \leq \text{T} \leq 40\text{K}$ and $\rho > 0.075\text{g/cm}^3$**

$$A = 0.538007\text{x}10^{-01} - 0.120407\text{x}10^{-02} * \text{T}$$

$$B = -0.253839\text{x}10^{+01} + 0.566168\text{x}10^{-01} * \text{T}$$

$$C = 0.449175\text{x}10^{+02} - 0.998152\text{x}10^{+00} * \text{T}$$

$$D = -0.353461\text{x}10^{+03} + 0.72285\text{x}10^{+01} * \text{T}$$

$$E = 0.104424\text{x}10^{+04} - 0.230085\text{x}10^{+02} * \text{T}$$

**$33\text{K} \leq \text{T} < 36\text{K}$** and **$\rho > 0.075\text{g/cm}^3$**

$$A = -0.275020\text{x}10^{-01} + 0.110212\text{x}10^{-02} * \text{T}$$

$$B = 0.117525x10^{+01} - 0.487800x10^{-01} * T$$

$$C = -0.184317x10^{+02} + 0.800791x10^{+00} * T$$

$$D = 0.124700x10^{+03} - 0.576384x10^{+01} * T$$

$$E = -0.302676x10^{+03} + 0.152884x10^{+02} * T$$

**$22K \leq T < 33K$** and $\rho > 0.075 g/cm^3$

$$A = 0.282191x10^{-01} - 0.155902x10^{-02} * T + 0.322665x10^{-04} * T^2$$

$$B = -0.131286x10^{+01} + 0.685339x10^{-01} * T - 0.139911x10^{-02} * T^2$$

$$C = 0.231542x10^{+02} - 0.113302x10^{+01} * T + 0.226347x10^{-01} * T^2$$

$$D = -0.184177x10^{+03} + 0.839441x10^{+01} * T - 0.162347x10^{+00} * T^2$$

$$E = 0.559566x10^{+03} - 0.236825x10^{+02} * T + 0.437404x10^{+00} * T^2$$

**$20K < T < 22K$** and $\rho > 0.077 g/cm^3$

$$A = -0.196538x10^{-01} + 0.128818x10^{-02} * T$$

$$B = 0.901540x10^{+00} - 0.613574x10^{-01} * T$$

$$C = -0.152179x10^{+02} + 0.108723x10^{+01} * T$$

$$D = 0.111263x10^{+03} - 0.847962x10^{+01} * T$$

$$E = -0.293960x10^{+03} + 0.245057x10^{+02} * T$$

**$17K \leq T \leq 20K$**

$$A = -0.446732x10^{-01} + 0.252585x10^{-02} * T$$

$$B = 0.224243x10^{+01} - 0.127828x10^{+00} * T$$

$$C = -0.420352x10^{+02} + 0.241908x10^{+01} * T$$

$$D = 0.348548x10^{+03} - 0.202838x10^{+02} * T$$

$$E = -0.107787x10^{+04} + 0.65617x10^{+02} * T$$

**$T < 17K$** and $\rho > \mathbf{0.075 g/cm^3}$

$$A = -0.853063x10^{-01} + 0.976589x10^{-02} * T - 0.247566x10^{-03} * T^2$$

$$B = 0.321564x10^{+01} - 0.356815x10^{+00} * T + 0.813185x10^{-02} * T^2$$

$$C = -0.392538x10^{+02} + 0.407149x10^{+01} * T - 0.682502x10^{-01} * T^2$$

$$D = 0.139394x10^{+03} - 0.107156x10^{+02} * T - 0.174518x10^{+00} * T^2$$

$$E = 0.194107x10^{+03} - 0.438586x10^{+02} * T + 0.301042x10^{+01} * T^2$$

Figure 6 shows the maximum error between the calculated values and the NBS table values for viscosity at temperatures below 100 K. The data fall below a 5% error with the majority below 2%. The curve fit was then compared to the tabular values for three significant pressures: atmospheric, critical, and supercritical. Figure 7 compares the predicted viscosity to the published values for hydrogen at one atmosphere pressure. The predicted values closely match the published values for both the liquid and gaseous phases. The correlation at the critical pressure is presented in Figure 8. Viscosity does not show a divergence at the critical point. Finally, the correlation at a supercritical pressure is shown in Figure 9. Here, the pressure was set to 1500 KPA or 1.16 times the

critical pressure. From the shape of the curves it is obvious why only a low density and a high-density region were required to provide an acceptable curve fit.

## Conclusion

The equations described in this paper provide an easy and accurate method of predicting the thermal conductivity and viscosity of hydrogen for temperatures below 100 K and pressures up to 1000 KPa. The FORTRAN program created by the NBS [5] was modified to include the equations described above. The computer program was then employed to perform a comparison of the pressure response of liquid hydrogen to the pressure response of liquid oxygen at their respective critical points.

## References


1. Garland, C. W. and Williams, R. D., "Low-frequency Sound Velocity Near the Critical Point of Xenon", *Phys. Rev. A*, 10-4 (1974), 1328
2. Hendricks, R. C., Baron, A. K. and Peller, I. C., "GASP - A Computer Code for Calculating the Thermodynamic and Transport Properties for Ten Fluids: Parahydrogen, Helium, Neon, Methane, Nitrogen, Carbon Monoxide, Oxygen, Fluorine, Argon, and Carbon Dioxide", *NASA Technical Note D-7808*, (1975)
3. Emanuel, G., "Introduction to Critical Point Theory with Application to Fluid Mechanics", *AIAA, 96-2,* (June 1996), 129
4. Nwobi, Obika C., Long, Lyle N. and Micci, Michael M., "Molecular Dynamics Studies of Properties of Supercritical Fluids", *Journal of Thermophysics and Heat Transfer*, 12-3, (July-September 1998), 322-327

5. McCarty, R. D., "Interactive Fortran IV Computer Programs for the Thermodynamic and Transport Properties of Selected Cryogens (Fluids Pack)", *NBS Technical Note 1025*, (1980)
6. Hanley, H. J., McCarty, R. D., and Intemann, H., "The Viscosity and Thermal Conductivity of Dilute Gaseous Hydrogen from 15 to 5000 K", *Journal of Research of the National Bureau of Standards – A. Physics and Chemistry*, 74A-3, (May – June 1970)
7. Roder, H. M., and Diller, D. E., "Thermal Conductivity of Gaseous and Liquid Hydrogen", *Journal of Chemical Physics*, 52-11, (1 June 1970)
8. McCarty, R. D., Hord, J., and Roder, H. M., "Selected Properties of Hydrogen (engineering design data)", *National Bureau of Standards*, (1981)
9. McCarty, R. D., "Thermophysical Properties of Helium-4 from 4 to 3000 R with Pressures to 15000 PSIA", *NBS Technical Note 622*, (September 1972)

Table 1 – Thermal Conductivity Curve Fit Coefficients

| | $40K < T < 75K$ | $33K \leq T \leq 40K$ | $32K \leq T \leq 40K$ | $T < 32K$ | $T \leq 22K$ |
|---|---|---|---|---|---|
| | Curve fit 1 | Curve fit 2 | Curve fit 3 | Curve fit 4 | Curve fit 5 |
| $X_1$ | $0.359343 \times 10^{-2}$ | $0.610708 \times 10^{-1}$ | $0.996513 \times 10^{+2}$ | $0.231879 \times 10^{-1}$ | $-0.302237 \times 10^{+1}$ |
| $X_2$ | $-0.320203 \times 10^{-3}$ | $-0.480935 \times 10^{-2}$ | $-0.670513 \times 10^{+1}$ | $-0.291474 \times 10^{-2}$ | $-0.654848 \times 10^{+0}$ |
| $X_3$ | $0.684352 \times 10^{-5}$ | $0.122292 \times 10^{-3}$ | $0.186958 \times 10^{+0}$ | $0.113756 \times 10^{-3}$ | $0.703479 \times 10^{-1}$ |
| $X_4$ | $-0.429492 \times 10^{-7}$ | $-0.101920 \times 10^{-5}$ | $-0.188593 \times 10^{-2}$ | $-0.144868 \times 10^{-5}$ | $-0.145155 \times 10^{-2}$ |
| $X_5$ | $-0.657379 \times 10^{+0}$ | $-0.904625 \times 10^{+2}$ | $-0.283875 \times 10^{+4}$ | $-0.571286 \times 10^{+1}$ | $0.169052 \times 10^{+3}$ |
| $X_6$ | $0.772415 \times 10^{-1}$ | $0.688178 \times 10^{+1}$ | $0.113848 \times 10^{+3}$ | $0.882118 \times 10^{+0}$ | $-0.291281 \times 10^{+1}$ |
| $X_7$ | $-0.196103 \times 10^{-2}$ | $-0.170487 \times 10^{+0}$ | $-0.448288 \times 10^{+1}$ | $-0.401339 \times 10^{-1}$ | $-0.474153 \times 10^{+0}$ |
| $X_8$ | $0.142554 \times 10^{-4}$ | $0.137255 \times 10^{-2}$ | $0.646446 \times 10^{-1}$ | $0.572794 \times 10^{-3}$ | $0.403391 \times 10^{-2}$ |
| $X_9$ | $0.147837 \times 10^{+3}$ | $0.217502 \times 10^{+5}$ | $0.149707 \times 10^{+5}$ | $-0.556360 \times 10^{+3}$ | $-0.129162 \times 10^{+3}$ |
| $X_{10}$ | $-0.180362 \times 10^{+2}$ | $-0.155565 \times 10^{+4}$ | $0.384486 \times 10^{+4}$ | $0.717611 \times 10^{+1}$ | $0.426176 \times 10^{+2}$ |
| $X_{11}$ | $0.490849 \times 10^{+0}$ | $0.350012 \times 10^{+2}$ | $-0.423525 \times 10^{+2}$ | $0.215320 \times 10^{+1}$ | $-0.556174 \times 10^{+1}$ |
| $X_{12}$ | $-0.376166 \times 10^{-2}$ | $-0.241006 \times 10^{+0}$ | $-0.403244 \times 10^{+0}$ | $-0.584037 \times 10^{-1}$ | $0.353707 \times 10^{+0}$ |

| | | | | | |
|---|---|---|---|---|---|
| $X_{13}$ | $0.291544 \times 10^{+5}$ | $-0.105106 \times 10^{+7}$ | $-0.110272 \times 10^{+7}$ | $0.524678 \times 10^{+6}$ | $-0.179205 \times 10^{+5}$ |
| $X_{14}$ | $-0.506066 \times 10^{+3}$ | $0.570871 \times 10^{+5}$ | $-0.525837 \times 10^{+5}$ | $-0.434403 \times 10^{+5}$ | $0.185432 \times 10^{+4}$ |
| $X_{15}$ | $-0.902909 \times 10^{+1}$ | $-0.514534 \times 10^{+3}$ | $0.719500 \times 10^{+3}$ | $0.101659 \times 10^{+4}$ | $-0.689358 \times 10^{+2}$ |
| $X_{16}$ | $0.148432 \times 10^{+0}$ | $-0.651237 \times 10^{+1}$ | $-0.487915 \times 10^{+1}$ | $-0.495007 \times 10^{+1}$ | $0.537557 \times 10^{+0}$ |
| $X_{17}$ | $-0.120000 \times 10^{+7}$ | $0.129222 \times 10^{+2}$ | $0.391219 \times 10^{+8}$ | $-0.668844 \times 10^{+1}$ | $-0.995309 \times 10^{+5}$ |
| $X_{18}$ | $0.241617 \times 10^{+5}$ | $0.122469 \times 10^{+7}$ | $-0.710429 \times 10^{+6}$ | $0.224704 \times 10^{+6}$ | $0.974862 \times 10^{+4}$ |
| $X_{19}$ | $0.272422 \times 10^{+3}$ | $-0.861367 \times 10^{+5}$ | $0.111144 \times 10^{+5}$ | $-0.346450 \times 10^{+4}$ | $-0.305666 \times 10^{+3}$ |
| $X_{20}$ | $-0.542153 \times 10^{+1}$ | $0.136533 \times 10^{+4}$ | $0.251145 \times 10^{+3}$ | $-0.150762 \times 10^{+3}$ | $-0.453023 \times 10^{+2}$ |
| $X_{21}$ | $0.113418 \times 10^{+8}$ | $0.697990 \times 10^{+1}$ | $-0.324325 \times 10^{+9}$ | $-0.416010 \times 10^{+1}$ | $-0.512421 \times 10^{+7}$ |
| $X_{22}$ | $0.257187 \times 10^{+5}$ | $-0.644070 \times 10^{+2}$ | $0.315749 \times 10^{+7}$ | $0.314617 \times 10^{+1}$ | $0.210300 \times 10^{+6}$ |
| $X_{23}$ | $-0.123460 \times 10^{+5}$ | $0.531457 \times 10^{+6}$ | $0.107766 \times 10^{+6}$ | $-0.279761 \times 10^{+0}$ | $0.113568 \times 10^{+5}$ |
| $X_{24}$ | $0.141239 \times 10^{+3}$ | $-0.933265 \times 10^{+4}$ | $-0.745936 \times 10^{+4}$ | $0.162868 \times 10^{+4}$ | $0.416300 \times 10^{+3}$ |
| $X_{25}$ | $0.504982 \times 10^{+0}$ | $0.000000 \times 10^{+0}$ | $0.137662 \times 10^{+3}$ | $0.000000 \times 10^{+0}$ | $0.765159 \times 10^{+8}$ |
| $X_{26}$ | $-0.357369 \times 10^{+7}$ | $-0.204210 \times 10^{+2}$ | $0.890544 \times 10^{+8}$ | $-0.402382 \times 10^{+1}$ | $-0.266769 \times 10^{+7}$ |
| $X_{27}$ | $0.146900 \times 10^{+6}$ | $-0.470943 \times 10^{+2}$ | $-0.287183 \times 10^{+7}$ | $-0.117582 \times 10^{+1}$ | $-0.146626 \times 10^{+6}$ |
| $X_{28}$ | $-0.141778 \times 10^{+4}$ | $-0.197265 \times 10^{+6}$ | $0.655508 \times 10^{+5}$ | $-0.904111 \times 10^{+1}$ | $-0.144348 \times 10^{+4}$ |
| $X_{29}$ | $-0.489403 \times 10^{+2}$ | $0.000000 \times 10^{+0}$ | $0.668644 \times 10^{+2}$ | $0.000000 \times 10^{+0}$ | $-0.379681 \times 10^{+3}$ |
| $X_{30}$ | $0.162709 \times 10^{+2}$ | $0.000000 \times 10^{+0}$ | $-0.340703 \times 10^{+3}$ | $0.105514 \times 10^{-7}$ | $-0.319721 \times 10^{+8}$ |
| $X_{31}$ | $-0.151925 \times 10^{+6}$ | $-0.553572 \times 10^{+2}$ | $-0.540557 \times 10^{+7}$ | $0.207713 \times 10^{+0}$ | $0.234894 \times 10^{+7}$ |
| $X_{32}$ | $0.245402 \times 10^{+4}$ | $0.314421 \times 10^{+7}$ | $0.120796 \times 10^{+4}$ | $-0.554118 \times 10^{+1}$ | $-0.231774 \times 10^{+5}$ |

Table 2. The effect of density correction for thermal conductivity

| Case | DC | AEBC | AEAC | STBC | SDAC | TSBC | TSAC | MEBC | MEAC |
|---|---|---|---|---|---|---|---|---|---|
| 1 | No | 0.097 | - | 0.40% | - | 1.3% | - | 0.88 | - |
| 2 | Yes | 0.13 | 0.0059 | 1.74 | 0.25 | 5.35 | 0.75 | 11.56 | 1.6 |
| 3 | No | 0.22 | - | 0.25 | - | 0.97 | - | 0.88 | - |
| 4 | - | 0.079 | - | 0.27 | - | 0.89 | - | 1.60 | - |
| 5 | Yes | 0.083 | 0.013 | 8.02 | 0.16 | 24.24 | 0.49 | 80.35 | 0.64 |
| 6 | Yes | 3.63 | 0.72 | 10.31 | 0.12 | 34.56 | 1.08 | 51.98 | 0.88 |
| 7 | No | 0.34 | - | 0.20 | - | 0.94 | - | 0.92 | - |
| 8 | Crit | 97.2 | 0.098 | - | - | - | - | - | - |
| 9 | - | 0.12 | - | 0.35 | - | 1.17 | - | 0.92 | - |
| 10 | Yes | 0.98 | 0.0002 | 6.03 | 0.19 | 19.07 | 0.57 | 28.7 | 0.93 |
| 11 | No | 0.022 | - | 0.26 | - | 0.80 | - | 0.72 | - |
| 12 | Yes | 0.16 | 0.0057 | 1.09 | 0.12 | 3.43 | 0.42 | 2.47 | 0.40 |
| 13 | - | 0.019 | - | 0.19 | - | 0.59 | - | 0.93 | - |

1- $75<T<100$

2- $40<T<75$ and $\rho \leq 0.06$, Curve fit 1

3- $40<T<75$ and $\rho \geq 0.06$

4- $40<T<75$ for all densities after correction

5- $32<40<40$ and $\rho<0.03143$, not including the critical point, Curve fit 2

6- $32<T<40$ and $0.03143<\rho<0.06$, not including the critical point, Curve fit 3

7- $32<T<40$ and $\rho>0.06$

8- Critical point

9- $32<T<40$ for all densities after correction

10- $T<32$ and $\rho \leq 0.03143$, Curve fit 4

11- $22<T<32$ and $\rho>0.06$

12- $T \leq 22$ and $\rho \geq 0.06$, Curve fit 5

13- $T<32$ for all densities

Table 3. The effect of density correction for viscosity

| Case | AEBC | AEAC | SDBC | SDAC | TSBC | TSAC | MEBC | MEAC |
|---|---|---|---|---|---|---|---|---|
| 1 | 12.79 | 0.24 | 11.47 | 0.29 | 47.2 | 1.11 | 43.65 | 0.93 |
| 2 | 18.07 | 0.46 | 14.59 | 0.49 | 61.84 | 1.93 | 53.63 | 1.72 |
| 3 | 20.99 | 0.12 | 16.7 | 0.80 | 71.09 | 2.52 | 58.51 | 4.36 |
| 4 | 18.28 | 0.28 | 14.22 | 0.64 | 60.94 | 2.20 | 56.05 | 5.04 |
| 5 | 12.98 | 2.17 | 8.37 | 0.47 | 38.09 | 3.58 | 31.07 | 3.06 |
| 6 | 7.33 | 0.90 | 5.62 | 0.27 | 24.19 | 1.71 | 20.27 | 1.57 |
| 7 | 3.16 | 0.50 | 1.96 | 0.11 | 9.04 | 1.07 | 9.60 | 0.74 |

1- $40<T\leq46$ and $\rho>0.075$

2- $36\leq T\leq40$ and $\rho>0.075$

3- $33\leq T<36$ and $\rho>0.075$

4- $22\leq T<33$ and $\rho>0.075$

5- $20<T<22$ and $\rho>0.077$

6- $17\leq T\leq20$ and $\rho>0.076$

7- $T<17$ and $\rho>0.075$

DC: Density Correction, %

AEBF: Average Error Before Correction, %

AEAC: Average Error After Correction, %

SDBC: Standard Deviation Before Correction, %

SDAC: Standard Deviation After Correction, %

TSBC: Three-sigma Before Correction, %

TSAC: Three-sigma After Correction, %

MEBC: Maximum Error Before Correction, %

MEAC: Maximum Error After Correction, %

Fig. 1 Maximum thermal conductivity error for 100 K and below

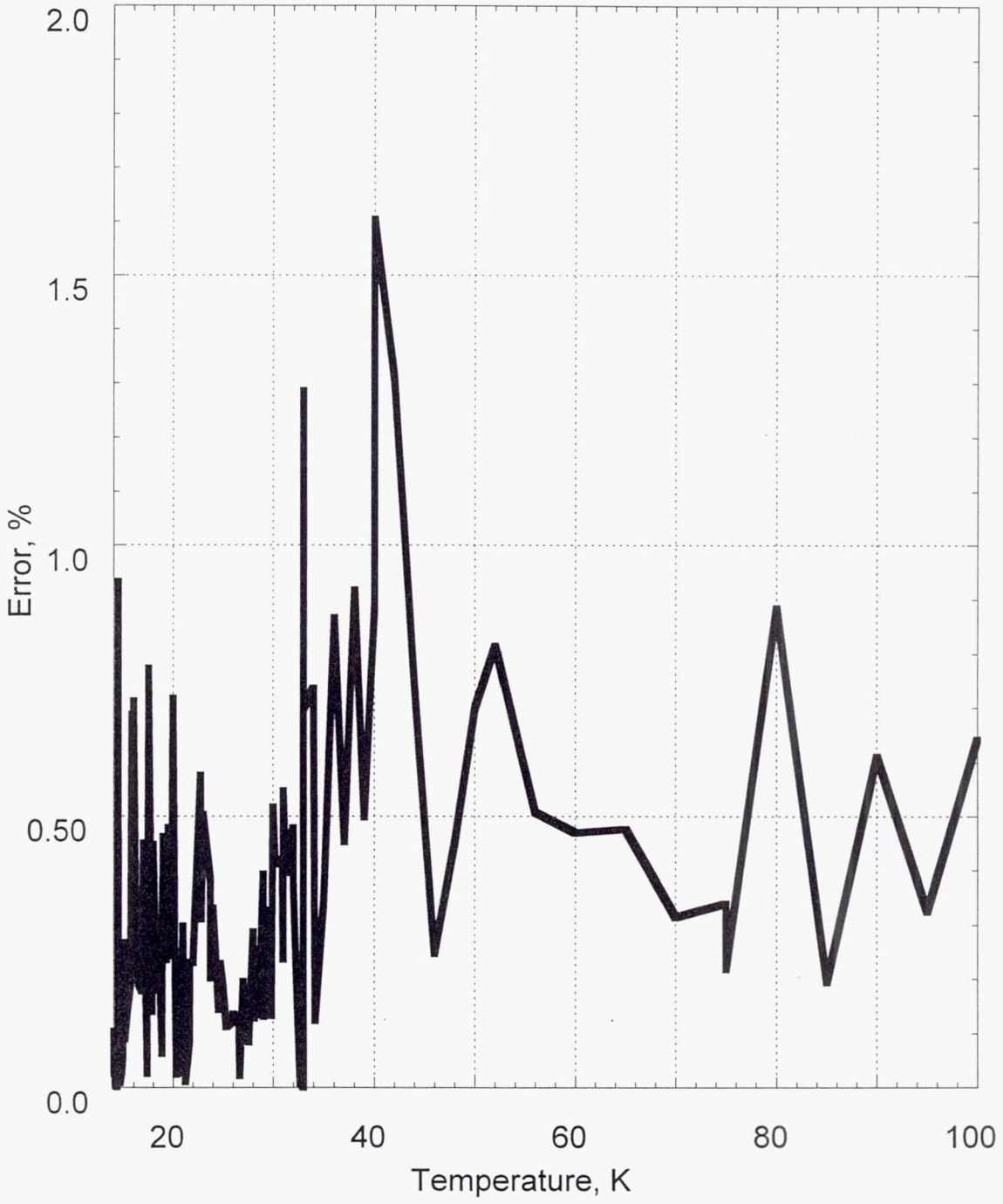

Fig. 2 Thermal conductivity at atmospheric pressure (101.325 KPa)

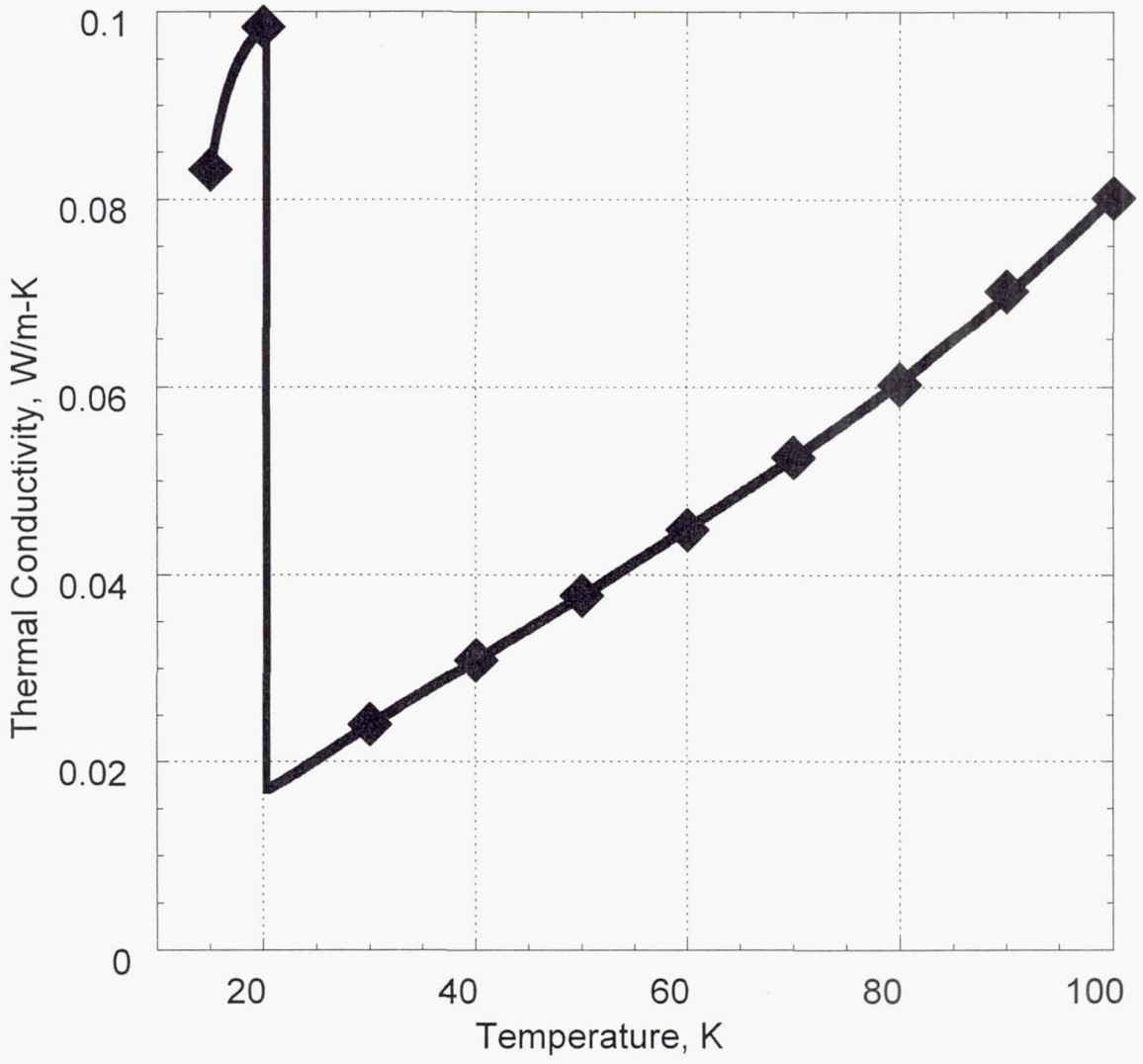

Fig. 3 Thermal conductivity at the critical pressure (1292.8 KPa)

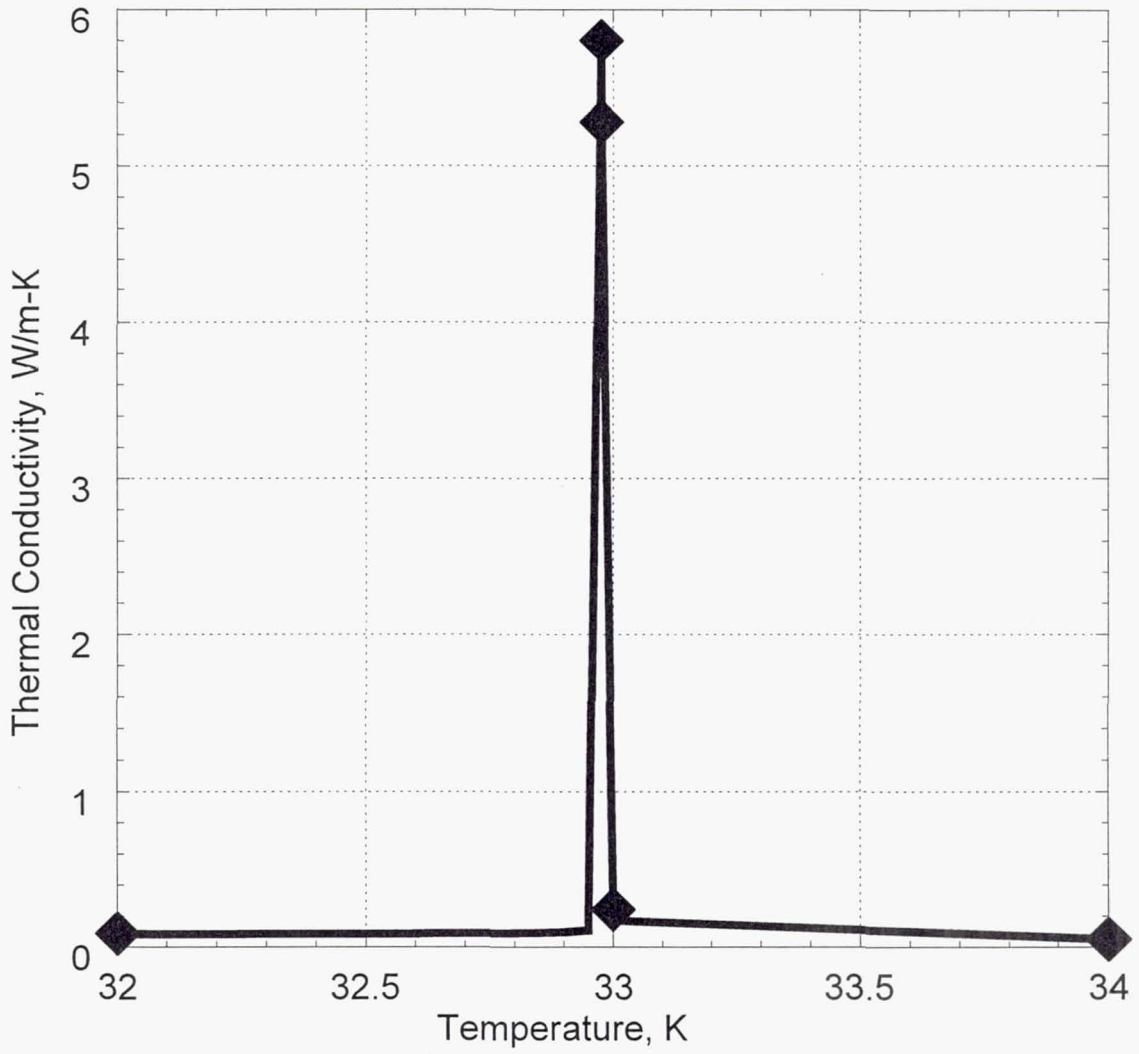

Fig. 4 Thermal conductivity at the supercritical pressure (1500 KPa)

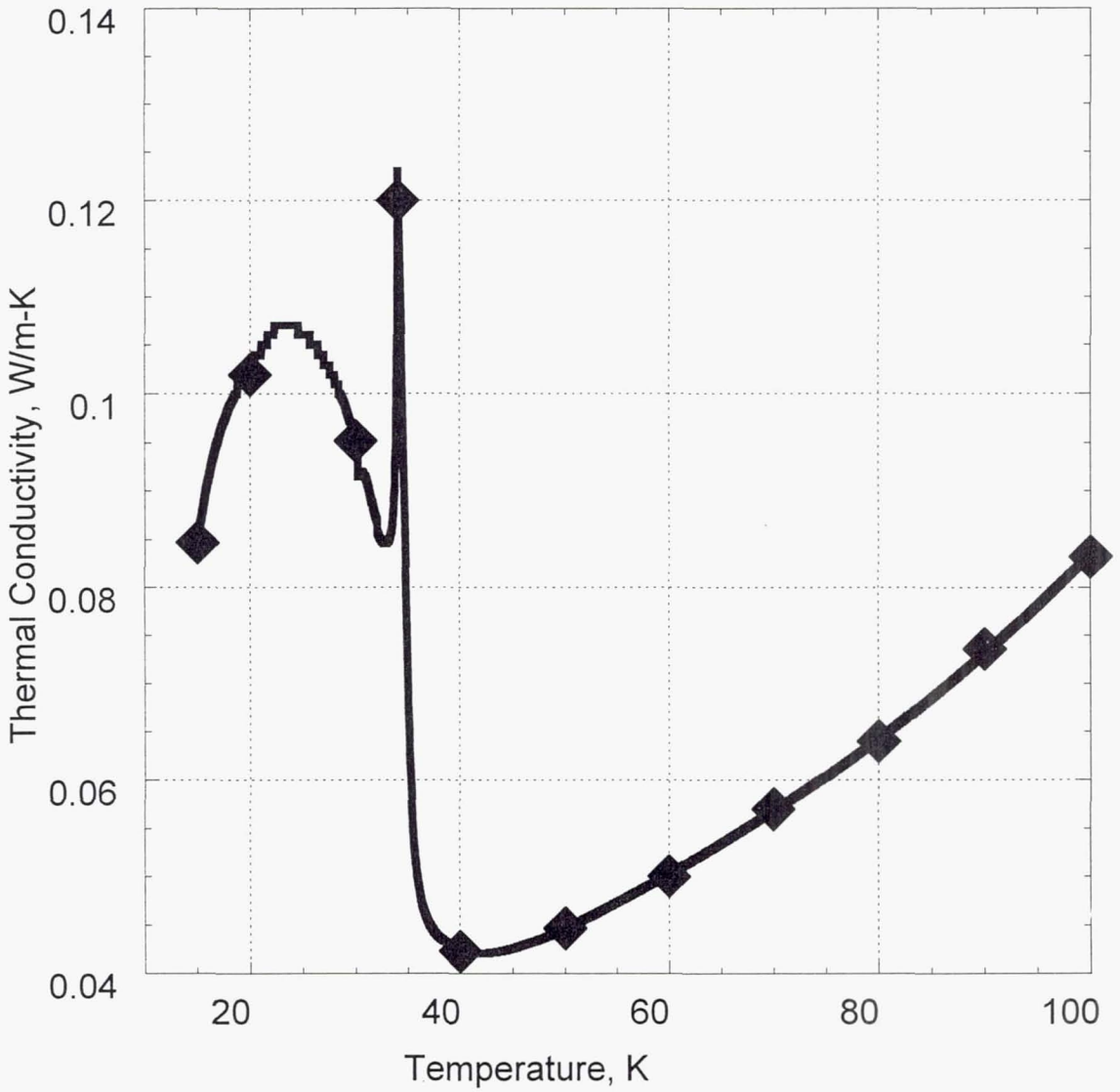

Fig. 5 Maximum viscosity error for 100 K and below

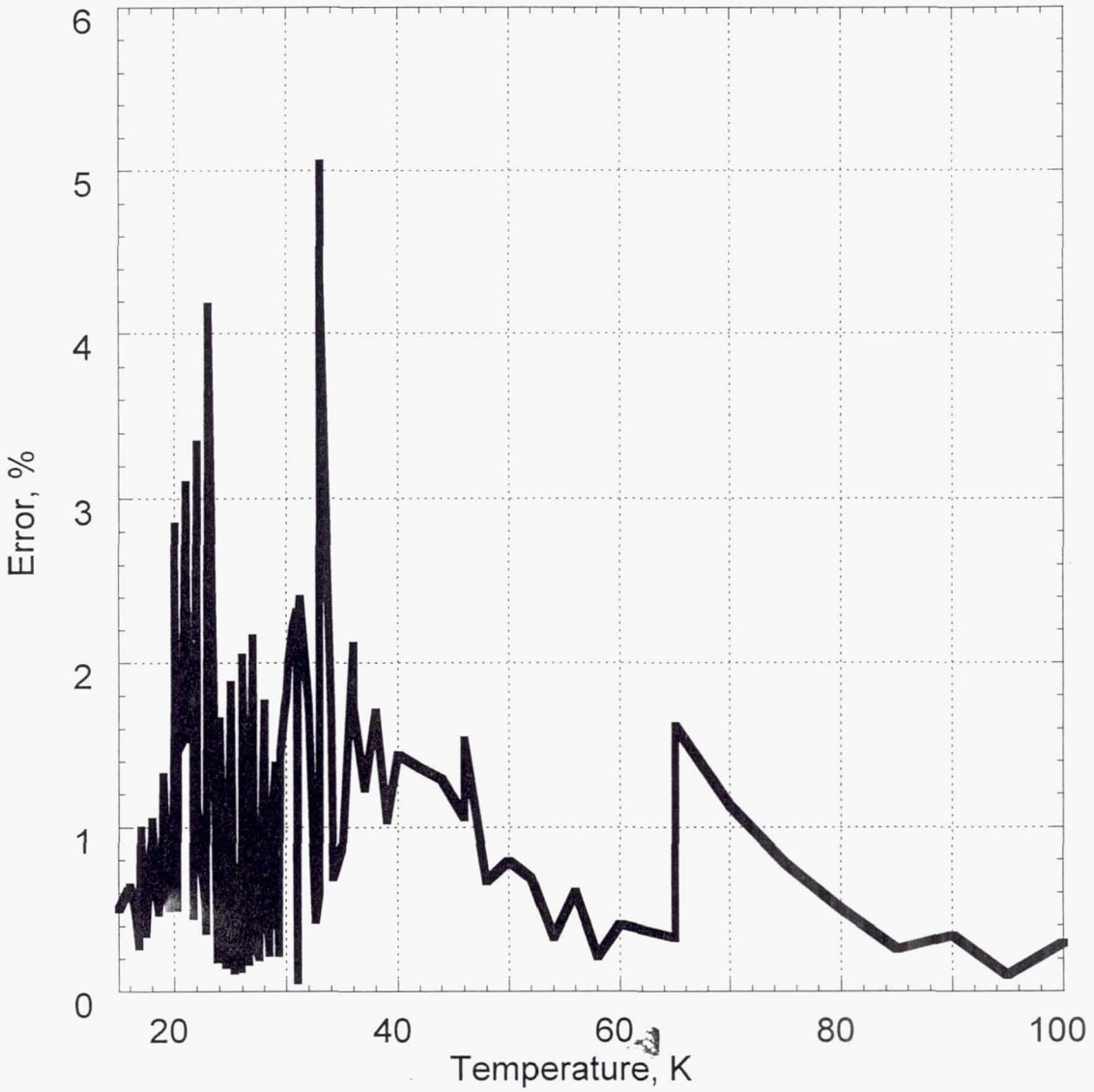

Fig. 6 Viscosity at atmospheric pressure (101.325 KPa)

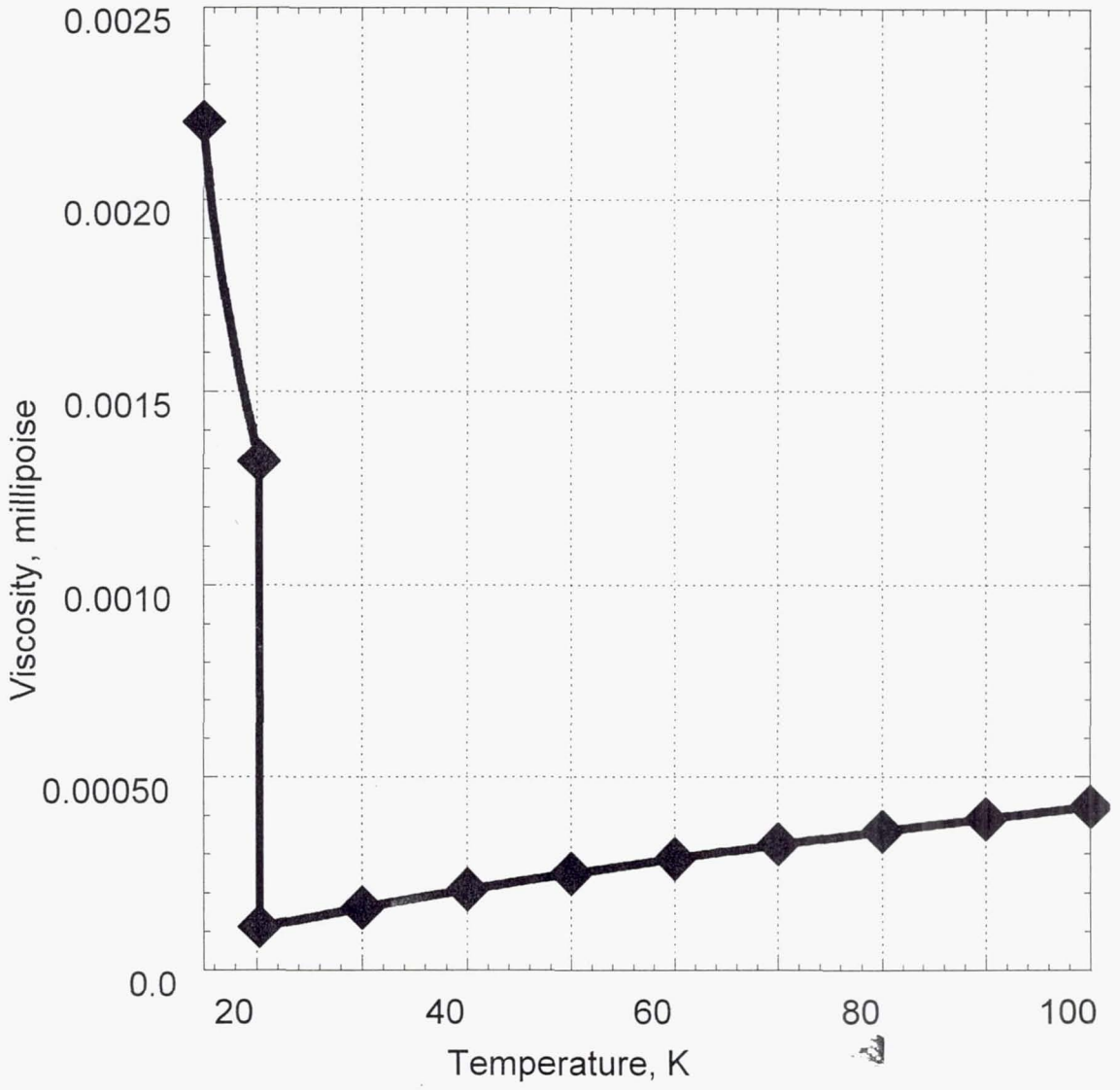

Fig. 7 Viscosity at the critical pressure (1292.8 KPa)

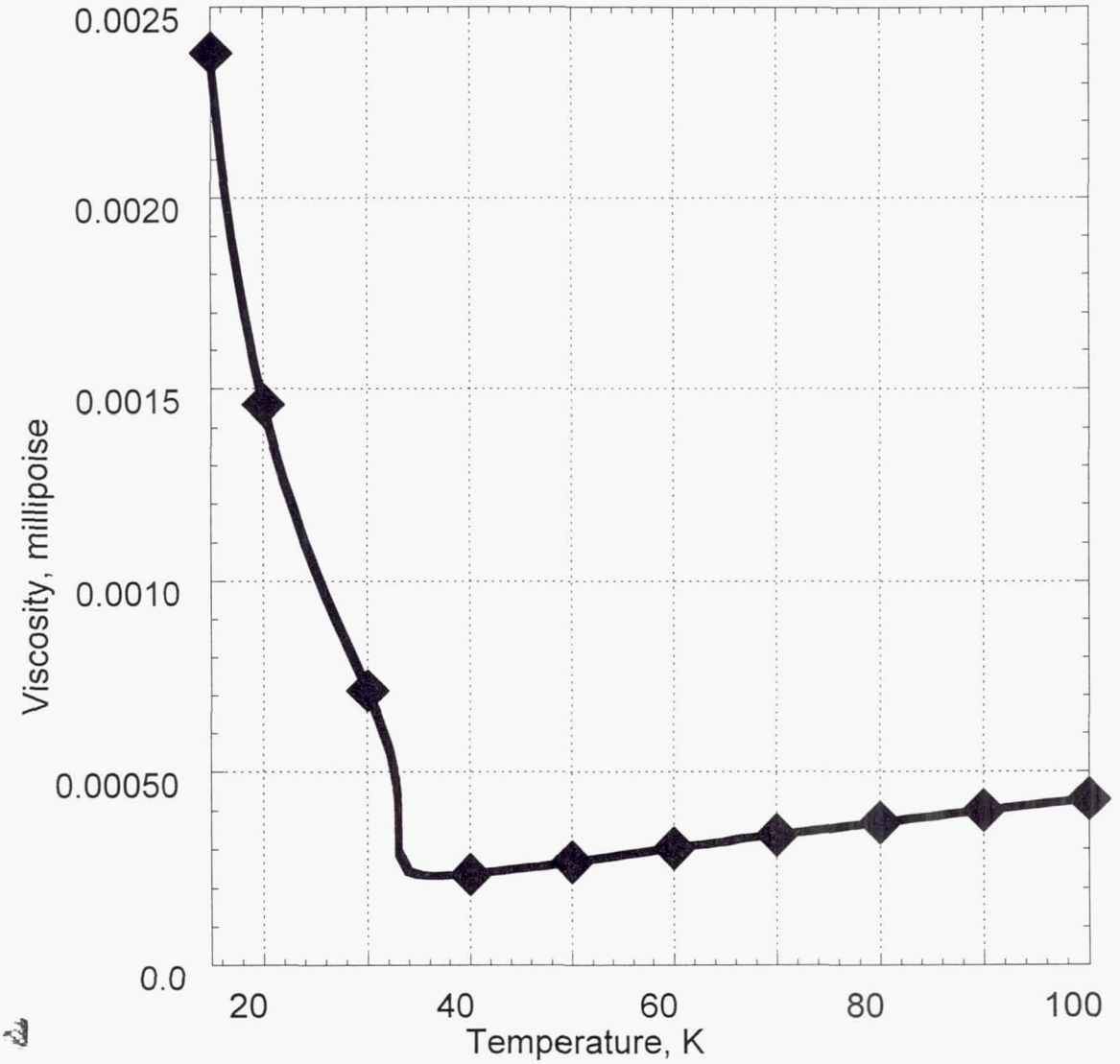

Fig. 8 Viscosity at the supercritical pressure (1500 KPa)